Available online at www.sciencedirect.com
SCIENCE DIRECT®
Optics Communications 260 (2006) 703–707
OPTICS COMMUNICATIONS
www.elsevier.com/locate/optcom

Population lensing effect in Cr:LiSAF probed by *Z*-scan technique

Nicolas Passilly, Elyes Haouas, Vivien Ménard, Richard Moncorgé, Kamel Aït-Ameur *

Center Interdisciplinaire de Recherche Ions Laser (CIRIL), UMR6637 CEA-CNRS-ENSICAEN et Université de Caen, 6 Bd. Maréchal Juin, F14050 Caen, France

Received 22 July 2005; received in revised form 5 October 2005; accepted 8 November 2005

Abstract

An experiment has been performed for measuring a nonlinear refractive index that is due to the polarizability difference $\Delta\alpha_P$ between excited ($^4T_2$) and ground ($^4A_2$) states in a Cr^{3+}:LiSAF crystal at $\lambda = 647$ nm. The latter one is responsible for a population lensing effect which has been monitored by using the eclipsing *Z*-scan technique. We have performed a data analysis that allows to distinguish between thermal and population contributions to the lensing effect. We have found $\Delta\alpha_P = 4.6 \times 10^{-25}$ cm^3 which is in a good agreement with our previous measurements with a different technique.

Keywords: Laser materials; Optically induced thermo-optical effects; Population lensing effect; Nonlinear lensing effect; *Z*-scan

1. Introduction

It has been recently shown that self-Q-switching operation can be obtained in a flash-lamp-pumped Cr^{3+}:LiSAF laser giving rise to a single pulse of several tens of millijoules and a few hundreds of nanoseconds [1]. This laser behavior has been modeled by resorting to a mechanism of intensity-dependent losses based on the combination of a hard aperture and a time-dependent lensing effect originating from the amplifying medium [2]. This nonlinear lensing effect is a population lensing effect assigned to a change of refractive-index Δn_{pop} of the amplifying material which has been initially assumed to be proportional to the Cr^{3+}-excited ion population density N_{ex}:

$$\Delta n_{pop}(r) = K\frac{N_{ex}(r)}{N_T}, \tag{1}$$

where $N_T = 1.3 \times 10^{20}$ cm^{-3} is the total density of Cr^{3+} ions and r is the radial coordinate [3,4]. In fact, authors of Ref. [3,4] have considered that Δn_{pop} was rather proportional to the inversion density N than to the upper level population density N_{ex}. It is important to note that in Ref. [3,4] the active medium was a ruby crystal for which N and N_{ex} are different since it is a three-level system. In our case, it is not necessary to distinguish between N and N_{ex} in Δn_{pop} since Cr^{3+}:LiSAF is a four-level system. By assuming that the radial variation of the Cr^{3+}-excited-state population density is only due to the saturation mechanism caused by the oscillating Gaussian mode, it results in that N_{ex} is minimum on the laser axis [5], as shown in Fig. 1(a). As a consequence, the population lens occurring in the laser material will be a converging effect for $K < 0$ and a diverging effect for $K > 0$.

The constant of proportionality K for Cr^{3+}:LiSAF has been experimentally measured from the time variation of the laser's far-field divergence [5] and has been found to be equal to $K = 5 \times 10^{-4}$.

The origin of the refractive-index change Δn_{pop} is attributed to a variation of ionic polarizability $\Delta\alpha_P = (\alpha_{ex} - \alpha_g)$ when the chromium ions change energy states as in many other host matrices [6–13]. As a result, the constant K defined by Eq. (1) takes the following explicit form [5,8]:

$$K = \frac{2\pi}{n_0} f_L^2 N_T \Delta\alpha_P, \tag{2}$$

where $n_0 = 1.4$ is the linear refractive index of the crystal when Cr^{3+} ions are not excited, and $f_L = (n_0^2 + 2)/3$ is

* Corresponding author. Tel.: +33 231 45 25 73; fax: +33 231 45 25 57.
E-mail address: kamel.aitameur@ensicaen.fr (K. Aït-Ameur).

0030-4018/$ - see front matter © 2005 Elsevier B.V. All rights reserved.
doi:10.1016/j.optcom.2005.11.019

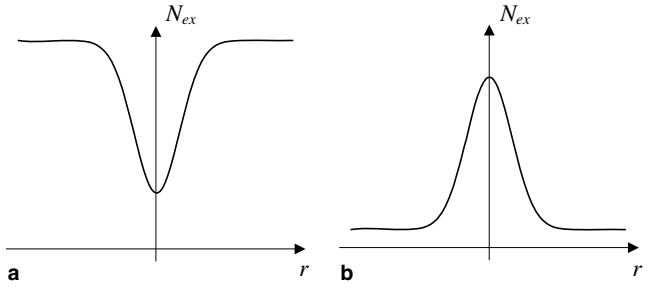

Fig. 1. Radial distribution of the population density of the excited level: (a) due to the saturation mechanism in a laser rod uniformly pumped by a lateral flashlamp; (b) due to longitudinal pumping caused by a Gaussian laser beam.

the Lorenz local field correction factor. Comparison of Eqs. (1) and (2) suggests to introduce a constant of proportionality C_K which does not depend upon the total density of Cr^{3+} ions contrary to constant K, and which can be expressed as $C_K = K/N_T = 3.8 \times 10^{-24}\,cm^3$. The refractive-index variation Δn_{pop} is then given by

$$\Delta n_{pop}(r) = C_K \cdot N_{ex}(r). \quad (3)$$

At the experimental value $K = 5 \times 10^{-4}$, it corresponds the value for the polarizability difference between the excited and ground state of Cr^{3+} ions in Cr^{3+}:LiSAF:$\Delta\alpha_P = 4.6 \times 10^{-25}\,cm^3$. This value seems to be the highest values of $\Delta\alpha_P$ measured in various Chromium doped materials [10] which have been found to vary from 10^{-26} to $10^{-25}\,cm^3$. A question arises now: Is this particular high value of $\Delta\alpha_P$ corresponds to an actual property of Cr^{3+}:LiSAF, or is due to systematic errors made in the data analysis in Ref. [5]? The latter is based on a laser cavity modeling which is grounded upon some approximations. The main of them was to approximate the radial Gaussian term, in the Cr^{3+}-excited ion population density N_{ex}, by a parabolic expression in order to describe the propagation inside the laser rod with standard *ABCD* formalism.

Our purpose in this study is to estimate again the value of $\Delta\alpha_P$ for Cr^{3+}:LiSAF, but with a method different from the one used in Ref. [5]. For that, we will consider a single-pass technique, the *Z*-scan method, which is widely used for determination of nonlinear refractive-index originating as well as from optical Kerr effect [14] or from population-lens effect [10].

2. Modeling of the experiment

2.1. Experimental set-up

The experimental *Z*-scan set-up involves a translation stage supporting the Cr^{3+}:LiSAF sample which is moved across the focal plane of a plano-convex lens of focal length $f = 70$ mm. We excited the Cr^{3+}:LiSAF, using a CW Kr^+-ion laser at $\lambda = 647.1$ nm, in resonance with $^4A_2 \rightarrow {}^4T_2$ transition centered at 650 nm. All the measurements were made with the laser polarization perpendicular to the *c*-axis oriented along the beam direction. The crystal has a thickness $L = 2$ mm and a total density of Cr^{3+} ions $N_T = 6.78 \times 10^{19}\,cm^{-3}$, experimentally determined from the measurement of its absorption coefficient which has been found equal to $1.34\,cm^{-1}$ at $\lambda = 647.1$ nm. The laser beam is Gaussian and used both as excitation beam and probe beam. It is characterized by a half divergence angle $\theta = 0.2$ mrad and a Rayleigh range z_0 of about 0.7 mm for the focused beam in the crystal. About 4% of the incident beam is split off using a simple glass plate and detected by a photodiode giving a voltage signal V_1 which is proportional to the power contained in the laser beam incident on the sample. The power variation of the transmitted beam is monitored by a second photodiode (voltage signal V_2), not through a diaphragm as usually, but through an obscuration disk, referred as a *stop* in the following, which eclipses most of the beam. This has been named the eclipsing *Z*-scan (EZ-scan) technique [15]; it allows a sensitivity enhancement in comparison with the use of a diaphragm. Another advantage of the EZ-scan technique is that the correct alignment of the stop is easily checked since the resulting pattern is a ring of light. The stop of radius $r_S = 1.98$ mm, set at a distance $D \gg z_0$, is characterized by the linear transmittance $S = \exp[-2r_S^2/W_S^2] = 0.135$, where $W_S = 1.98$ mm is the $1/e^2$ width of the Gaussian beam incident on the stop when the crystal sample is removed. The stop is characterized by its transmission T_s which is proportional to the ratio V_2/V_1. The normalized transmission T_n is obtained from the value of T_s measured with a crystal sample normalized to the value of T_s without sample. The experimental EZ-scan data are shown in Fig. 2 for a CW input power of about 0.5 W. Before to proceed, it is important to note that the lensing effect under study is converging since, for the sample positioned prior to focus ($z < 0$), the far-field beam divergence increases, so that more light passes the stop, i.e., T_n is increased. When sample is set beyond the focal plane ($z > 0$), the lens effect

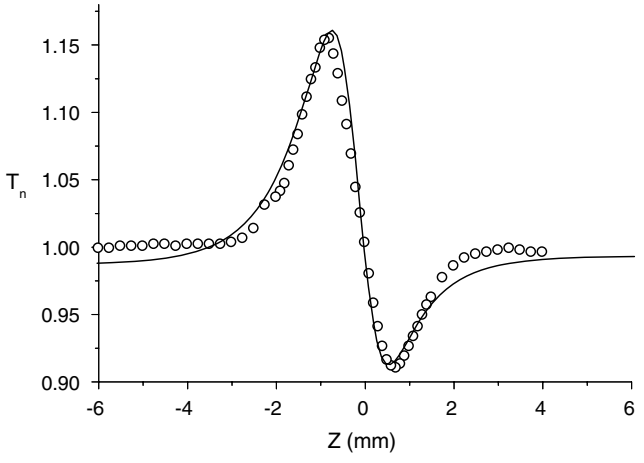

Fig. 2. Normalized Eclipsing *Z*-scan of a 2 mm-thick *c*-cut Cr^{3+}:LiSAF sample performed for a pump beam power of 500 mW at $\lambda = 647.1$ nm which is used both as excitation beam and as a probe beam; (○○○), experiment; (—), simulation for $C_K = 4.7 \times 10^{-24}\,cm^3$.

generated in the sample tends to collimate the beam so that the stop transmission reduces. Note that usual Z-scan technique based on the power transmission of a diaphragm should give exactly the opposite, that is a decrease (increase) of T_n when the sample is set before (after) the focal plane. It is important to note that we have found that the lensing effect in the EZ-scan experiment for Cr^{3+}:LiSAF is a converging effect while it was a diverging effect in Ref. [5]. These two results are not inconsistent because the transverse profile of N_{ex} for the EZ-scan experiment is maximum on the axis as shown in Fig. 1(b).

2.2. Thermal and population lensing effects

The absorption of the relative intense excitation beam generates two kinds of lensing effects. The first one is the population lens (PL) under study, and the second one is a thermal lensing (TL) caused by heat deposition by means of nonradiative relaxation processes of absorbed energy. As a consequence, the lensing effect displayed in Fig. 2 is due to the PL and TL contributions which have to be distinguished. The particularity of Cr^{3+}:LiSAF material is that thermal and population effects are very difficult to discriminate experimentally by using, for instance, a pulsed pump beam. This is because of the existence of a strong link between excited population and temperature distributions. The latter is due to upconversion and thermal quenching which are added to the usual quantum defect as sources of heat in the crystal as it will be discussed below.

In order to distinguish between thermal and population contributions, one has to estimate the temperature profile $T(r,z)$ imposed by the heat deposition in the crystal and heat removal from the cooled copper heat sink on which the crystal is in contact. In the steady-state, the temperature distribution $T(r,z)$ inside the crystal is given by the solution of heat conduction equation in cylindrical coordinates [16]:

$$\frac{\partial^2 T}{\partial r^2}+\frac{1}{r}\frac{\partial T}{\partial r}+\frac{\partial^2 T}{\partial z^2}+\frac{Q(r,z)}{K_c}=0, \tag{4}$$

where $K_c = 3\ \mathrm{Wm^{-1}\,K^{-1}}$ is the thermal conductivity of the crystal.

It is assumed that the heat flux is essentially radial and integration of Eq. (4) is made following the same method used in Ref. [16] except that, for Cr^{3+}:LiSAF, there are three heating sources [17,18] which contributes in the thermal power density $Q(r,z)$:

$$Q(r,z)=\frac{hc}{\lambda_l}\left[\left(\frac{\lambda_l}{\lambda_p}-1\right)W_p(r,z)+\gamma_{up}N_{ex}^2(r,z)+\frac{N_{ex}(r,z)}{\tau_{NR}(r,z)}\right]. \tag{5}$$

The first term in brackets in Q expression describes the usual quantum defect, where $\lambda_l = 850$ nm is the laser wavelength, $\lambda_p = 647.1$ nm the pumping wavelength, $W_p(r,z)$ is the pumping rate corresponding to the number of Chromium ions arriving in the upper state of laser transition per unit volume and per second.

The second term corresponds to the upconversion contribution, where $\gamma_{up} = 4.66\times10^{-16}\ \mathrm{cm^3/s}$ [19] is the upconversion parameter.

The third term describes the thermal quenching contribution in which $\tau_{NR}(r,z)$ is the nonradiative lifetime depending on temperature $T(r,z)$ [20]:

$$\tau_{NR}(r,z)=\tau_{NR}^0\exp\left(\frac{\Delta E}{kT(r,z)}\right), \tag{6}$$

where $\tau_{NR}^0 = 2.4\times10^{-14}$ s [20], $\Delta E = 5125\ \mathrm{cm^{-1}}$ [20] is the activation energy and k is the Boltzmann constant.

As pointed out above, one can see that determination of the excited population density N_{ex} is needed both for evaluating the PL and TL effects. At steady-state regime, we obtain the following expression [17] for the population density of the excited level $^4T_2$,

$$N_{ex}(r,z)=\frac{\sqrt{1+4\gamma_{up}\tau^2(r,z)W_p(r,z)}-1}{2\gamma_{up}\tau(r,z)}, \tag{7}$$

where $\tau(r,z)$ is the upper-state lifetime including radiative part (τ_f) and nonradiative part (τ_{NR}) so that:

$$\frac{1}{\tau(r,z)}=\frac{1}{\tau_f}+\frac{1}{\tau_{NR}(r,z)}. \tag{8}$$

For determining the dependence of N_{ex} and Q with coordinates r and z, we take into account the pump beam spreading inside the crystal since its Rayleigh range $z_0 = 0.7$ mm is lower than the crystal thickness $L = 2$ mm. In addition, pump-saturation effects have been accounted [21]. The longitudinal evolution of $T(r,z)$ and $N_{ex}(r,z)$ is determined in $m = 100$ slices of the crystal length. The thermal quenching of excited level fluorescence complicates slightly the determination of $T(r,z)$ and $N_{ex}(r,z)$ since the lifetime τ depends on temperature $T(r,z)$ and inversely.

This is an usual self-consistent problem which is easily to overcome by using iterative calculations [17]. This coupling between $T(r,z)$ and $N_{ex}(r,z)$, due to thermal quenching and upconversion mechanisms, does not make easy the discrimination between electronic and thermal contributions in the refractive-index variation, as done in Ref. [10]. The results for our crystal (0.8% doped) excited by a pump beam with a CW power of 500 mW shows that the temperature increase calculated in the focal plane is of about 11 °C with respect to the sample boundary assumed to be at a constant known temperature.

The following step is to evaluate the resulting optical path change Δs_{th} due to a temperature rise $\Delta T(r)$ [10,22]:

$$\Delta s_{th}(r)=L\frac{ds}{dT}\Delta T(r), \tag{9}$$

where ds/dT represents the temperature coefficient of the optical path length of the sample:

$$\frac{ds}{dT}=(n_0-1)(1+\nu)\gamma_L+\frac{dn}{dT}. \tag{10}$$

The value of the material parameters are as follows: $\nu = 0.3$ [19] is the Poisson's ratio, $\gamma_L = -10\times10^{-6}\ \mathrm{K^{-1}}$ ($\|c$) [19] is

the thermal expansion coefficient, and $dn/dT = -2.5 \times 10^{-6}\,K^{-1}$ ($\perp c$) [23] is the temperature coefficient of the refractive index.

After passing through the crystal, the laser beam is phase-shifted by a quantity obtained from the summation of the phase-shift introduced by each of the m slices:

$$\Delta\phi(r) = \frac{2\pi L}{m\lambda}\sum_{i=1}^{m}\left[\frac{\Delta s_{th}(i)}{L} + \Delta n_{pop}(i)\right]. \quad (11)$$

It is important to note that for Cr^{3+}:LiSAF, Δn_{pop} is positive while Δs_{th} is negative.

As pointed out above, the laser beam does not have a constant section along the crystal axis so that the thin sample approximation ($z_0 \gg L$) is not valid. It results in that usual Gaussian decomposition theoretical approach [14] cannot be applied to describe our experimental results.

3. Results and discussion

Now after getting the phase profile $\Delta\phi(r)$, it remains to determine the transmission of the stop. For that, we consider the far-field distribution $E_s(r)$, at the stop plane, resulting from the diffraction of the incident Gaussian beam passing through the phase aberration $\Delta\phi(r)$. The far-field distribution $E_s(r)$ is then numerically calculated by using the Fresnel–Kirchhoff integral. Finally, the stop transmission T_n normalized to the stop transmission without the crystal, is given by:

$$T_n = \frac{\int_{r_s}^{\infty}|E_s(r)|^2 r\,dr}{S\int_0^{\infty}|E_s(r)|^2 r\,dr}. \quad (12)$$

The simulation is organized as follows: for each position z of the crystal, we determine: (i) the thermal and population contributions for an arbitrary value of constant C_K; (ii) the transmission T_n. After that, we do the comparison between theoretical and experimental curves, T_n as a function of z, for several values of C_K. The best fit with the experimental plot gives us the value of C_K. Fig. 2 shows that a good agreement between theory and experiment has been achieved for

$$C_K = 4.7 \times 10^{-24}\,cm^3, \quad (13)$$

which corresponds to a polarizability difference $\Delta\alpha_P = 5.6 \times 10^{-25}\,cm^3$.

Now, let us consider the weight of the thermal contribution in comparison to the population effect in a EZ-scan experiment involving a Cr^{3+}:LiSAF crystal. For that, let us consider the quantity ΔT_n which represents the peak to valley transmittance difference. First, we determine numerically ΔT_n(pop), using Eq. (11) in which Δs_{th} is set to zero, which represents the population contribution to the EZ-scan curve. Secondly, the thermal contribution ΔT_n(th) is calculated using Eq. (11) in which Δn_{pop} is set to zero. It is important to note, that the link between temperature and population discussed in Section 2.2 is taken into account in the estimation of ΔT_n(pop) and ΔT_n(th). Fig. 3 shows the variation of ratio ΔT_n(pop)/ΔT_n(th) as a function of the doping level, and as expected, it is found that thermal contribution in the EZ-scan experiment increases with the doping level, i.e with the absorbed power. This behavior can be easily understood if one takes into account the influence of thermal quenching and upconversion mechanisms both on temperature increase and decrease of N_{ex}. Note that Fig. 3 has been plotted for three values of the doping level which are usually encountered in the literature.

Discrimination between population and thermal contributions to the nonlinear refractive-index measured with a Z-scan experiment is generally desirable [10] and can be achieved by using a pulsed pump beam. Another possibility, suggested through Fig. 3, for reducing TL contribution, is to make the EZ-scan experiment with a Cr^{3+}:LiSAF crystal having a low doping level allowing the use of a CW pump beam. This is the case for our experiment since the doping level is only 0.8%, and that corresponds, as shown in Fig. 3, to a population lensing effect ΔT_n(pop) of about four times the thermal contribution ΔT_n(th).

The value of $\Delta\alpha_P$ for Cr^{3+}:LiSAF previously obtained from Ref. [5], and confirmed in this work seems to be the highest values of $\Delta\alpha_P$ measured in various Chromium doped materials [10]. This interesting property should make easy the generation of refractive-index modulation which is useful for a laser oscillator based on a self-starting adaptative gain-grating resonator [24], or for holographic lasers where the laser medium is used as a phase-conjugate mirror [25,26]. Note that self-starting behavior has been demonstrated [27] with Nd:YAG laser which is characterized by a value of $\Delta\alpha_P$ ten times smaller than that for Cr^{3+}:LiSAF.

Now, it is interesting to compare the population lensing effects occurring in two Chromium doped materials. Indeed, it has been experimentally observed that the sign of the population lensing effect in Cr^{3+}:Al_2O_3 (ruby) [28]

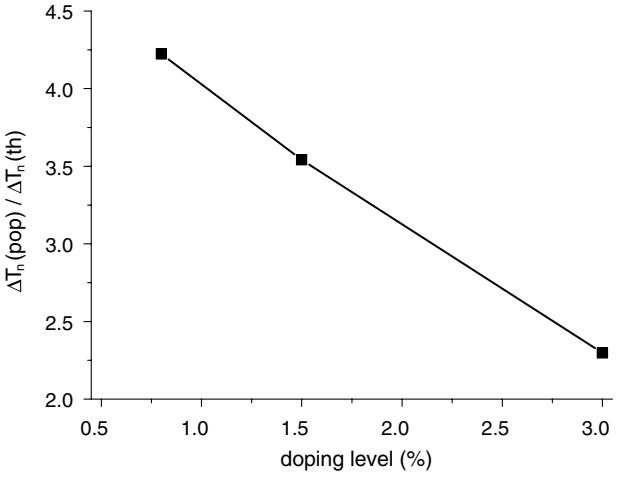

Fig. 3. Variations of ratio ΔT_n(pop)/ΔT_n(th) as a function of the Cr^{3+}:LiSAF doping level for a pump beam power of 500 mW at $\lambda = 647.1$ nm. ΔT_n represents the difference between the peak and valley transmittances determined theoretically for the TL and PL contributions.

is different from the one observed in Cr^{3+}:LiSAF [5], with similar experimental conditions. The latter are mainly:

– a plano-concave cavity;
– a laser rod uniformly pumped by lateral flashlamps;
– a free running behavior;
– a Gaussian oscillating mode.

Note that the population lensing effect in ruby [28] and Cr^{3+}:LiSAF has been monitored with the same technique described in details in Ref. [5]. In fact, the sign of the refractive-index change in ruby associated with a change in population inversion has been experimentally observed among a long time [3,4], and confirmed later in Ref. [28]. The present work has confirmed the sign of the refractive-index change in Cr^{3+}:LiSAF obtained in Ref. [5], but with a different technique. Now, a question arises: does $\Delta\alpha_P$ is positive for Cr^{3+}:LiSAF, and negative for Cr^{3+}:Al_2O_3? Since, the population lensing effect has been found to be converging [28] in Cr^{3+}:Al_2O_3, and diverging [5] in Cr^{3+}:LiSAF, with similar experimental conditions, one could deduce that the sign of $\Delta\alpha_P$ is different for the two materials.

Many measurements of $\Delta\alpha_P$ in ruby can be found in the literature [6–9,11,29], but unfortunately the different techniques used are not able to specify the sign of $\Delta\alpha_P$:

(i) The authors of Ref. [6] used an interferometric technique which gives the absolute value of Δn_{pop}.
(ii) The use of degenerate four wave mixing allows the knowledge of the square of $\Delta\alpha_P$ [7,11].
(iii) The determination of $\Delta\alpha_P$ from the far-field patterns resulting from the diffraction due to self-phase modulation [8] is not able to state its sign. Indeed, the diffraction of a Gaussian beam by a phase aberration $\varphi(r)$ or $-\varphi(r)$ leads to the same far-field pattern.
(iv) The two-wave mixing technique [29] is based on the measurement of the diffraction efficiency of a phase grating induced in the material, and this neither can give the sign of the phase modulation.

The Z-scan technique is in principle able to give the sign of the refractive-index change Δn_{pop}. It has been applied to ruby material by authors of Ref. [9]. They reported a positive value for Δn_{pop} in contrast with experiments involving ruby as a laser oscillator [3,4,28]. A possible explanation of this discrepancy is that the ruby material was in a regime of saturable absorber in Ref. [9], and in a regime of amplifier in [3,4,28]. Indeed, since the ruby material is a three-level system, its population inversion density N is negative in Ref. [9] while it is positive in [3,4,28]. We think that this property of the population inversion is in position to justify the sign difference in Δn_{pop} found for ruby material in various experiments. As a matter of fact, as pointed out in Section 1, Δn_{pop} is rather proportional to the population inversion density N than to N_{ex} [3,4,8]. However, in the case of a four-level material as Cr^{3+}:LiSAF, it is usual to approximate N by N_{ex}. In conclusion, we think that the question about the sign of the polarisability difference between excited and ground state in Chromium doped materials needs further investigations in order to be clarified.

References

[1] B.C. Weber, A. Hirth, Opt. Commun. 149 (1998) 301.
[2] M. Fromager, K. Aït-Ameur, Opt. Commun. 191 (2001) 305.
[3] D.A. Berkley, G.J. Wolga, J. Appl. Phys. 38 (1967) 3231.
[4] A. Flamholz, G.J. Wolga, J. Appl. Phys. 39 (1968) 2723.
[5] N. Passilly et al., J. Opt. Soc. Am. B 21 (2004) 531.
[6] T. Catunda, J.P. Andreeta, J.C. Castro, Appl. Opt. 25 (1986) 2391.
[7] T. Catunda, J.C. Castro, Opt. Commun. 63 (1987) 185.
[8] T. Catunda, L.A. Cury, J. Opt. Soc. Am. B 7 (1990) 1445.
[9] L.C. Oliveira et al., Jpn. J. Appl. Phys. 35 (1996) 2649, Part 1.
[10] A.A. Andrade et al., J. Opt. Soc. Am. B 16 (1999) 395.
[11] S.C. Weaver, S.A. Payne, Phys. Rev. B 40 (1989) 10727.
[12] R.C. Powell, S.A. Payne, Opt. Lett. 15 (1990) 1233.
[13] C.R. Mendonça et al., Phys. Rev. B 56 (1997) 2483.
[14] M. Sheik-Bahae, A.A. Said, T.H. Wei, D.J. Hagan, E.W. Van Stryland, IEEE J. Quantum Electron. 26 (1990) 760.
[15] T. Xia et al., Opt. Lett. 19 (1994) 317.
[16] M.E. Innocenzi et al., Appl. Phys. Lett. 56 (1990) 1831.
[17] F. Balembois et al., IEEE J. Quantum Electron. 25 (1997) 269, and comments and corrections;
IEEE J. Quantum Electron. 33 (1997) 1614.
[18] J.M. Eichenholz, M. Richardson, IEEE J. Quantum Electron. 34 (1998) 910.
[19] S.A. Payne, L.K. Smith, R.J. Beach, B.H.T. Chai, J.H. Tassano, L.D. DeLoach, W.L. Kway, R.W. Solarz, Appl. Opt. 33 (1994) 5526.
[20] M. Stalder, M. Bass, B.H.T. Chai, J. Opt. Soc. Am. B 9 (1992) 2271.
[21] G. Martel, C. Ozkül, F. Sanchez, Opt. Commun. 185 (2000) 419.
[22] J. Wei, F. Gan, Opt. Commun. 219 (2003) 261.
[23] S.A. Payne, W.F. Krupke, L.K. Smith, W.L. Kway, L.D. DeLoach, J.B. Tassano, IEEE J. Quantum Electron. 28 (1992) 1188.
[24] B.A. Thompson, A. Minassian, R.W. Eason, M.J. Damzen, Appl. Opt. 41 (2002) 5638.
[25] A. Brignon, L. Loiseau, C. Larat, J.-P. Huignard, J.-P. Pocholle, Appl. Phys. B 69 (1999) 159.
[26] S.Y. Lam, M.J. Damzen, Opt. Commun. 218 (2003) 365.
[27] O.L. Antipov, N. Eremeykin, A.P. Savikin, V.A. Vorob'ev, D.V. Bredikhin, M.S. Kuznetsov, IEEE J. Quantum Electron. 39 (2003) 910.
[28] K. Aït-Ameur, T. Kerdja, D. Louhibi, J. Phys. D: Appl. Phys. 15 (1982) 1667.
[29] S.C. Zilio, J.C. Penaforte, E.A. Gouveia, M.J.V. Bell, Opt. Commun. 86 (1991) 81.